Pool boiling performance of finned surfaces in R-113

N. Abuaf, S. H. Black and F. W. Staub*

Performance of horizontal copper heaters with a transverse fin structure was investigated for pool boiling heat transfer and critical heat flux limits. Data were obtained for 5.1 and 7.6 cm diameter structured copper and brass heaters in saturated R-113 boiling at pressures ranging between 0.037 and 1 atm. The fin structure consisted of 0.16 cm × 0.16 cm × 0.32 cm high square fins with an inter-fin spacing of 0.16 cm. Following a similar methodology to Haley and Westwater[1], a numerical analysis of the heat transfer phenomenon was performed by solving the one-dimensional fin conduction equation with a non-linear heat transfer boundary condition obtained from the previously reported data for R-113 boiling on plain surfaces. The predictions agreed with the data at the 1 atm pressure levels but showed deviations at the low pressure levels. The results showed that, compared with plain surface heaters of the same diameters the finned structured surfaces investigated: (a) decreased the wall temperature differences for a given heat flux and saturated pool boiling conditions, thus improving the nucleate boiling heat transfer coefficients, and (b) increased the critical heat flux limits, calculated as the power input divided by the heater projected area, by a factor of 2–2.5.

Keywords: *heat transfer, boiling, critical heat flux, finned surface, R-113*

Miniaturization of electronic components, accompanied by an increase in the required heat fluxes dissipated to values of 100 W/cm^2, have forced packaging engineers to search for non-conventional advanced cooling techniques. Saturated pool boiling is one of the available methods that can be easily adapted to compact systems. In the optimal application of this method, the two elements of information necessary are the steady-state junction or element temperature, and the critical heat flux limit. For a given dissipated power level, the component temperatures are required to be as low as possible for reliable operation. The critical heat flux limit, on the other hand, determines the maximum power that can be dissipated and is required to be as high as possible for a prescribed margin of safety.

Several thorough reviews of boiling heat transfer augmentation techniques have been published recently[2–4]. Since the present work involved boiling from finned surfaces, we present a brief review on the use of extended fins to enhance the nucleate boiling heat transfer coefficients. Massive fins were applied to the immersion cooling of high power density electronic tubes by the 'Vapotron' technique[5]. The boiling process along the fin was observed to be temperature controlled resulting in various boiling regimes occurring simultaneously along the fin. The performance characteristics of boiling heat transfer from single fins, finned tubes, and multiple parallel cylindrical fins extending into the boiling liquid were investigated by Haley and Westwater[1], Bondurant and Westwater[6], and Westwater[7]. Haley and Westwater[1] applied the heat conduction analysis to boiling fins with non-linear boundary conditions taking into consideration all the boiling regimes that are expected to occur along the fin, and extended the results to determine the optimum cylindrical fin shape and geometry. The predictions were in good agreement with their experimental results obtained at atmospheric pressures. The cylindrical fins investigated by Westwater and his students were 0.64 cm in diameter and 1.91 cm long. Although the clearance distance between the fins located in the same row was changed from 0 to 0.23 cm, the distance between two rows of fins was kept at 1 cm[7]. Their results showed the existence of an optimal inter-fin distance below which the vapour bubbles entrapped between the fins reduced the thermal performance.

The purpose of the present study was to investigate the characteristic boiling curves and critical heat flux limits of boiling surfaces consisting of a structure of square fins located at even intervals and covering the whole surface of the heater block under atmospheric and subatmospheric pressures, and to compare their performance with the solution of the non-linear fin equation.

Experimental

The experimental pool boiling rig used during the present study is the same as the one described in detail by Abuaf and Staub[8]. The set-up (Fig 1) consists of a steel test vessel and a glass test section that can be operated independently. The 15.2 cm diameter, 30.5 cm long glass vessel is connected by standard flanges to two stainless-

* Engineering Systems Laboratories, GE Corporate Research and Development, PO Box 8, Schenectady, New York 12301, USA
Received 23 April 1984 and accepted for publication on 6 September 1984

steel transition pieces. The top and bottom transition pieces incorporate the ports for the exit of the vapour, return of the liquid from the condenser, and for the instrumentation to measure the saturated pool conditions. The R-113 vapour exits the test sections through vertical risers and is condensed in a 316 stainless steel shell and tube condenser. A non-condensable gas separator is connected to the top of the condenser and can be evacuated by means of a steam ejector. The condensate returns by gravity at the bottom of the test sections. The shell side of the condenser is cooled by a 50% ethylene glycol, 50% water mixture flowing in a forced convection loop. The coolant loop temperature is controlled either by a river water cooled heat exchanger or by a coil immersed in a dry ice alcohol bath. The existing valve and bypass capabilities allow an accurate control of the condenser coolant inlet temperature.

Fig 2(a) is a schematic of the glass test section. Four copper-constantan thermocouples are used to monitor the pool temperature. Two of them are in the vapour and two in the liquid. The pool pressure is measured by a 0–1.4 atm variable inductance pressure transducer. The heater surface penetrates into the pool through a brass base and a high temperature plastic flange. Two rows of four cartridge heaters, rated for 500 W each, are energized by a 220 V, 8 kW variable power supply. The power is monitored by a wattmeter with a 0.25% accuracy. The heater block is heavily insulated with glass wool to minimize heat losses. Viton 'o' rings compatible with R-113 are used in the system connections and between the heater block and the plastic flange. Three separate finned heater surfaces were tested, two made of copper and one made of brass. The 5.1 cm diameter, 6.1 cm long copper heater was tested in the glass test section while the 7.6 cm heater was tested in the steel vessel. The 5.1 cm diameter 3.1 cm long brass heater was tested in the glass test section.

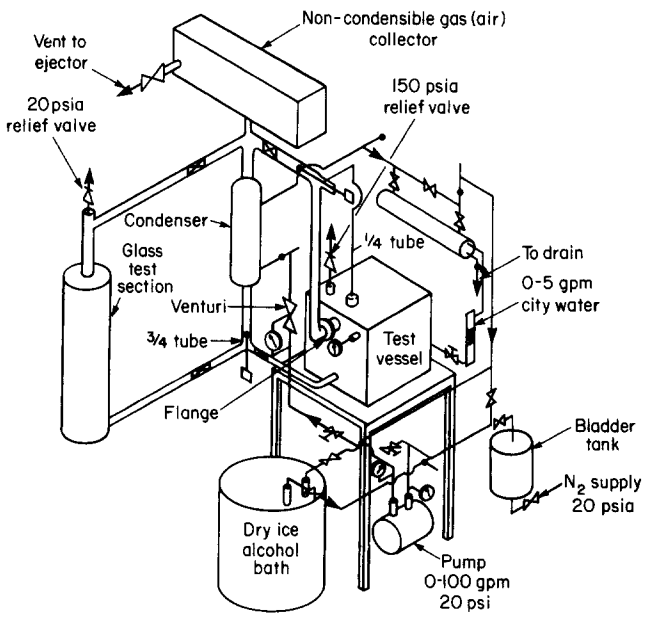

Fig 1 Experimental pool boiling rig

Detail of the heater blocks with the finned top surfaces is given in Fig 2(b). The 0.16 cm long, 0.16 cm wide and 0.32 cm high square fin matrix is machined on the top surface of the heaters. The distance between two adjacent fins is 0.16 cm in both orthogonal directions. Eight calibrated chromel alumel thermocouples are used to measure the axial temperature profiles along the heater blocks. Two of the thermocouples are positioned near the cylindrical heater periphery at two axial locations in order to monitor the radial temperature variations. The axial heat fluxes calculated from the axial temperature profiles were within 1% of the power meter readings.

The test liquid used was R-113. The free surface level was maintained approximately 10 cm above the heated surface. Since the results of the present study should be applicable to industrial applications, no special effort was made to polish and clean the heater finned surfaces after every run or change the R-113 regularly.

The experimental procedure followed was similar to Abuaf and Staub's[8]. It consisted of purging the system of non-condensibles and bringing the pool to the desired saturation conditions. Once these conditions were obtained, the power level was increased at regular intervals and instruments were monitored to check that steady state operation conditions were reached. All the instruments were connected to a Fluke datalogger, and data were recorded at 10 minute intervals; steady state

Notation

A	Fin cross-sectional area
g	Acceleration due to gravity
Gr	Grashof number, $\frac{g\theta L_h}{\nu^2 T_s}$
h	Heat transfer coefficient
h_{fg}	Latent heat of vaporisation
k	Thermal conductivity of fin material
k_l	Thermal conductivity of liquid phase
L_b, L_f	Axial length of base below fin and fin respectively (see Fig 7)
L_h	Heater width
Nu	Nusselt number, $\frac{hL_h}{k_l}$
P	Perimeter
Pr	Prandtl number, $\frac{c\mu}{k_l}$
q	Heat flux
q_L	Critical heat flux as determined by Lienhard's[1]
q_R	Critical heat flux as determined by Rohsenow[11]
q_Z	Critical heat flux as determined by Zuber[9]
T_w, T_s	Temperature of heater wall and saturated pool respectively
x	Axial distance of fin from reference point (See Fig 7)
μ	Dynamic viscosity of liquid phase
ν	Kinematic viscosity of liquid phase
ρ_l, ρ_g	Density of liquid and vapour phase respectively
σ	Liquid surface tension
θ	$T_w - T_s$

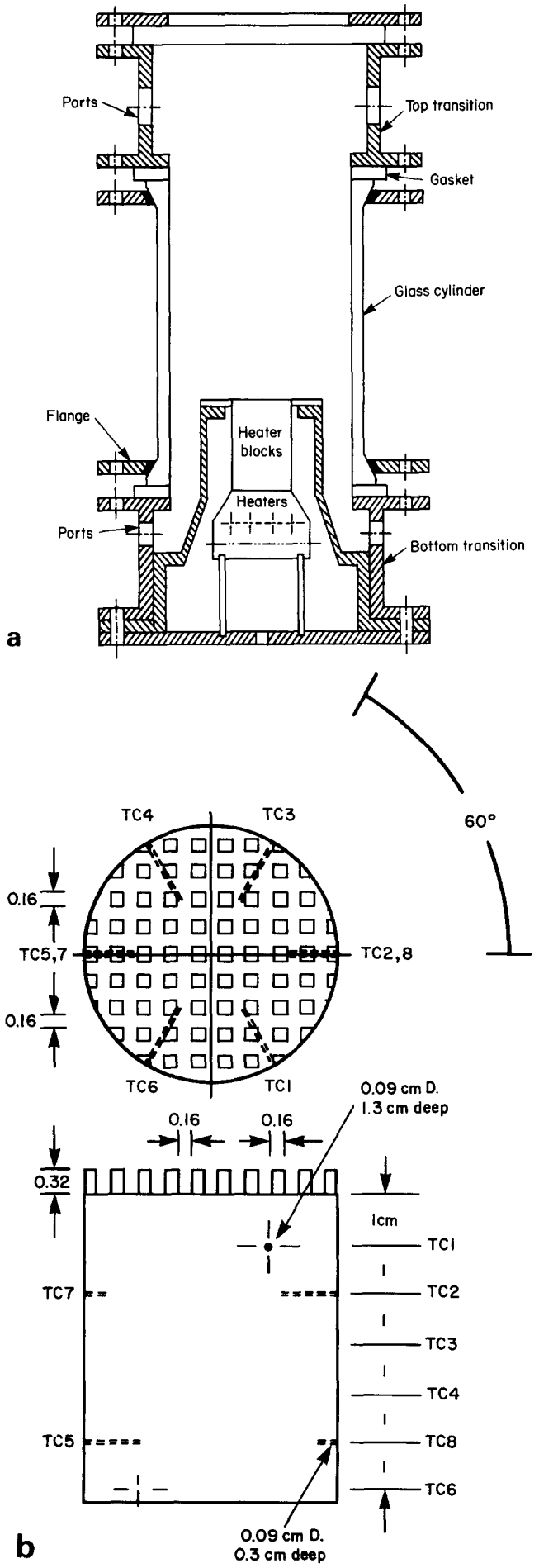

Fig 2(a) Glass test section and (b) heater blocks

was reached when three consecutive readings did not change by more than 0.2°C. Since the initiation of nucleate boiling occurred around the periphery of the heater between the flange and the heater block due to the 'o' ring, data were recorded only at high heat fluxes when most of the heater surface was already covered with nucleation sites. The critical heat flux limits were recorded as the point where a continuous rise of the heater temperatures was observed and no steady-state conditions could be attained. An automatic thermostat, set at 175°C, prevented the overheating of the heater blocks by automatically turning the power off.

Results

Pool boiling curves

Pool boiling curves of heat flux plotted against temperature difference between the wall and the saturated pool for the 7.6 cm and 5.1 cm copper heaters are given in Fig 3. The wall temperatures, defined as the fin base temperatures, were determined from the six temperatures measured. A mean square line was fitted through the data points and extrapolated to the axial location of the fin base. The heat flux was defined as the total power input divided by the projected cross-sectional area of the cylindrical heaters. Fig 3(a) depicts the boiling curves obtained from the 7.6 and 5.1 cm finned copper heaters at atmospheric pressure and 48.3°C pool temperature (saturated conditions). Four boiling curves obtained with the 5.1 cm finned copper heater are presented in Fig 3(b) covering a saturation pool pressure range between 0.037 and 0.89 atm. The data represent the boiling curve regions covering the nucleate boiling regime up to the critical heat flux limit. They do not include the single-phase convection regime or the overshoot which is usually observed before the onset of nucleation.

In Fig 3(b) it is shown that for the same heat flux level, the pool boiling curves for the finned surfaces in R-113 shift to the right, ie to higher values of the temperature difference between the wall and the pool, as the operating pressure is decreased. This observation is similar to that reported by Abuaf and Staub[8] for boiling on plain copper surfaces. The difference between the boiling curves for the plain surface and the finned surface heater is associated with the fact that for the same heat flux, the wall-to-pool temperature differences recorded with the finned surfaces are lower than the ones measured with the plain surface. Higher nucleate boiling heat transfer coefficients occur with the finned surfaces than with the plain surfaces.

Fig 4 shows the reproducibility of the boiling curve results for the 0.89 atm pressure runs performed after a period of three weeks of successive operation. For the same heat flux value the results are reproducible within a band of plus minus 1.5°C. Fig 3(a) depicts the reproducibility of the boiling curves at atmospheric pressure for two heater diameters (5.1 and 7.6 cm) from tests performed in the test vessel and in the glass test section. The scatter in this case is slightly larger but still within a few degrees centigrade. Similar boiling curves were also recorded for the 5.1 cm diameter brass finned heater at pool pressures of 1, 0.88, 0.39 and 0.14 atm. Fig 5 depicts the boiling curves obtained with the brass finned surface at the two pressure limits of 1 and 0.14 atm.

Critical heat flux limits

The critical heat flux limits measured on the 5.1 and 7.6 cm diameter finned copper heaters in the pressure range between 0.039 and 1 atm are presented in Fig 6. On the same figure the critical heat flux limits obtained with a 5.1 cm diameter plain surface copper heater in R-113[8] are also presented for comparison. The reader is reminded that the critical heat flux limits for the plain surface agreed with the Zuber[9], Kutateladze[10] expression with a constant value of 0.18 proposed by Rohsenow[11], for pressures above 0.3 atm. Below 0.3 atm the predicted values continue to decrease while the measured values level off. On average the critical heat flux limits obtained with the finned copper surfaces are around 2.4 times higher than the plain surface results. The variation of the critical heat flux limit with pool pressure is similar to the one observed with the plain surface. The data first decrease with the pool saturation pressure between 1 and 0.3 atm, and for pressure levels below 0.3 atm the dependance of the critical heat flux on the pool pressure becomes less and follows a trend similar to that of the plain surface. In the same figure the critical heat flux limits measured with the 7.6 cm diameter finned heater in the steel vessel are also plotted. The agreement between the two sets of data is quite reasonable.

The critical heat flux limits recorded with the 5.1 cm diameter finned brass heater in the pressure range between 1 and 0.14 atm in R-113 were 10 to 20% lower than those reported above for the finned copper heaters.

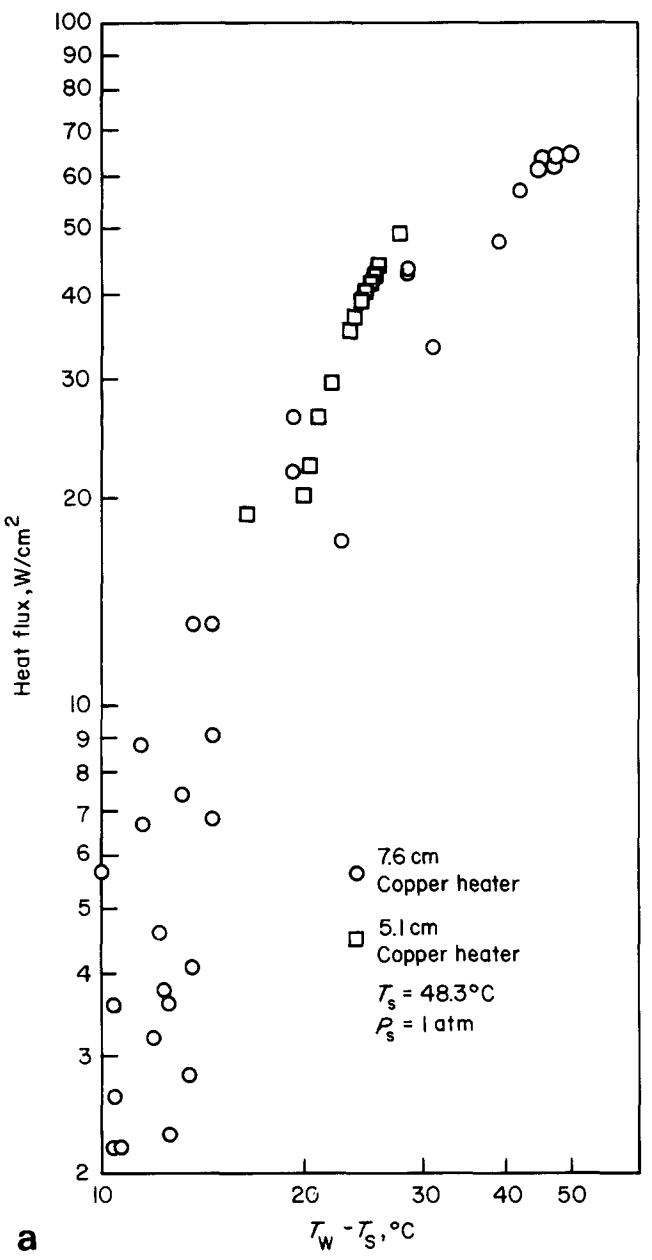

Fig 3 Pool boiling curves with copper heaters

Analytical calculations

Analytic predictions of the boiling curves for the finned surface were also attempted by following a fin analysis with a temperature-dependent heat transfer coefficient as proposed by Haley and Westwater[1], Bondurant and Westwater[6], Lai and Hsu[12] and Dulken et al[13]. The physical model presented in Fig 7(a) is a single fin with a portion of the copper base. The fin is usually considered one-dimensional and represented by the schematic in Fig 7(b). The one-dimensional fin equation with the temperature-dependent heat transfer coefficient for a plain surface may be written as:

$$\frac{d^2\theta}{dx^2} = \frac{h(\theta)P}{kA}\theta \qquad (1)$$

where $\theta = T_w - T_s$ is the temperature difference between the heater wall and the saturated pool, P the perimeter, A the cross-sectional area of the fin, k is the thermal conductivity of the fin material and x is the axial distance. The boundary conditions for the problem involve a specified temperature or heat flux below the fin base

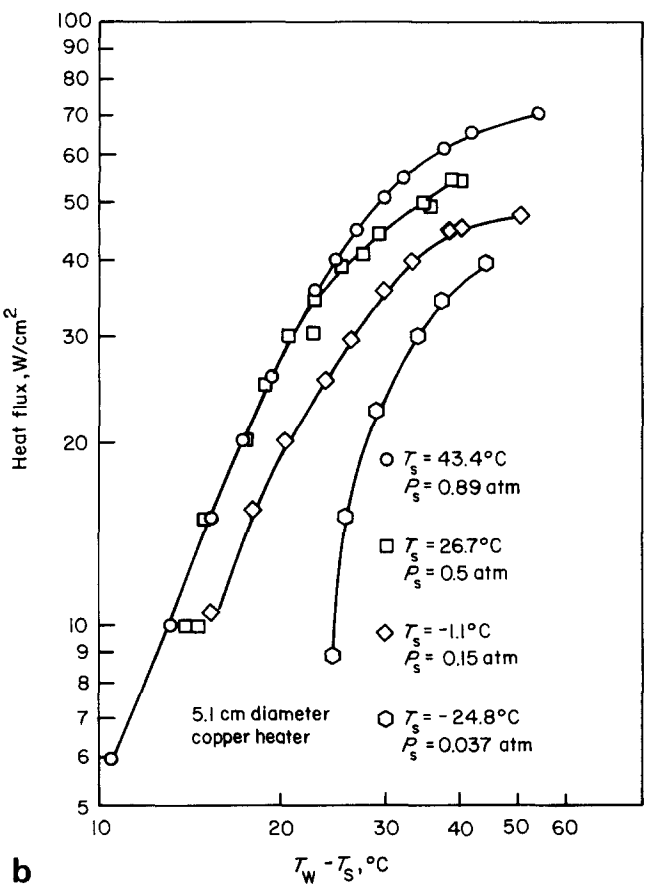

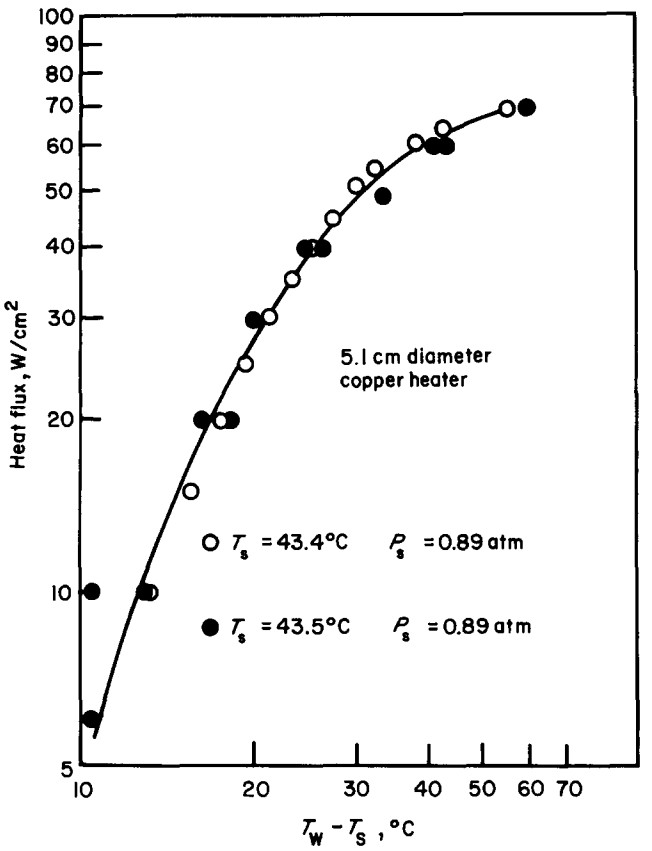

Fig 4 Reproducibility of pool boiling curves

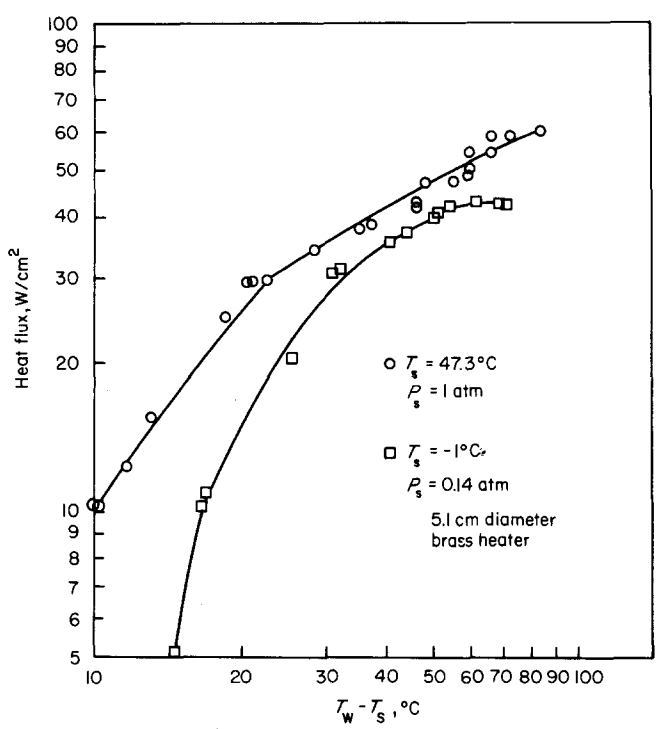

Fig 5 Pool boiling curves with brass heaters

($x=0$) and convective heat loss from the fin base ($x=L_b$), along the fin and at the top of the fin ($x=L_b+L_f$).

$$\theta=\theta_b \quad \text{at} \quad x=0 \tag{2}$$

$$-k\frac{d\theta}{dx}=h(\theta)\theta \quad \text{at} \quad L_b \leqslant x \leqslant L_b+L_f \tag{3}$$

The numerical solution applied for the one-dimensional problem was by successive over-relaxation of a finite-difference temperature array. The analysis provided the temperature profiles and the base heat flux for the chosen finned geometry in R-113.

Experimental pool boiling curves for finned surfaces have been obtained at atmospheric and subatmospheric pressures. In order to compare them with the model presented above, a good knowledge of the heat transfer coefficients of a plain surface as a function of temperature at several pressure levels is essential in all the regimes of the classical boiling curve, ie convection, nucleate boiling, transition region and film boiling. The model also needs the temperatures at which the transitions from one regime to the other occurs.

First we shall discuss the results obtained at pressures close to atmospheric. As specified above, the heat transfer coefficient curves had to be obtained from other sources for the free convection, nucleate boiling, transition and film boiling regimes. Fig 8 represents a compendium of the R-113 boiling heat transfer data available from the literature.

For the free convection regime of an upward facing heated surface, the recommended correlation[14] is:

$$Nu=C(GrPr)^{0.33} \tag{4}$$

The proposed value of the constant C varies from 0.14 (Collier[14]) to 0.32 (Lippert and Dougall[15]). For the present calculations, the value of 0.32 was chosen since it

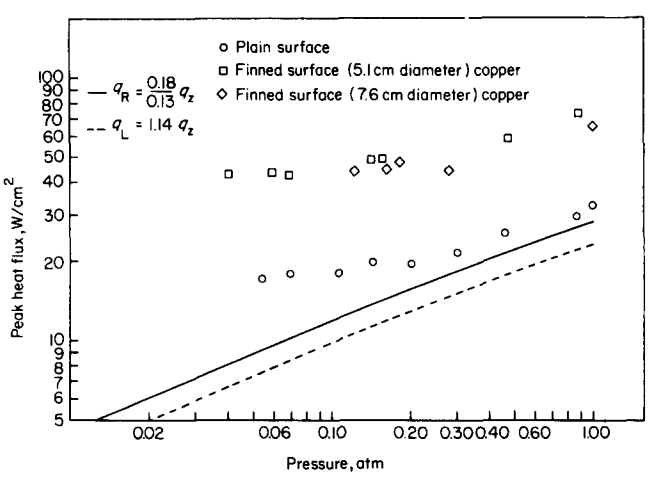

Fig 6 Critical heat flux limits

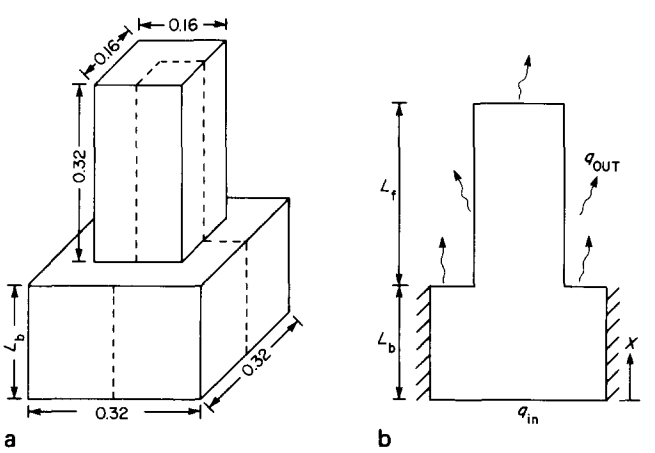

Fig 7 (a) Physical model of a single fin and (b) one dimensional representation

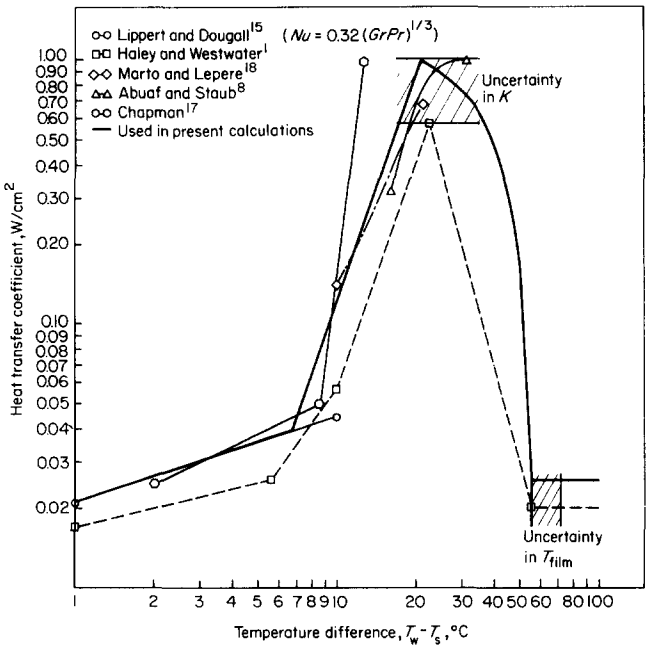

Fig 8 Published R-113 boiling heat transfer data

was determined by the above authors with R-113.

For the nucleate boiling region the empirical expression proposed by Stephan and Abdelsalam[16]:

$$h = B(\Delta T)^{2.92} \tag{5}$$

was used. For R-113 the value of the constant B depends on the pressure and for pool pressures above 0.2 atm the functional dependance proposed by Stephan and Abdelsalam was used since it was found[8] to predict the nucleate boiling curves for plain surfaces at pressures above 0.2 atm. The experimental data obtained by Chapman[17], Marto and Lepere[18] and Abuaf and Staub[8] presented in Fig 8 for R-113 at atmospheric pressure show some scatter when compared with the above expression. This may be due to the fact that Haley and Westwater[11] and Marto and Lepere[18] used copper tubes while Lippert and Dougall[15], Chapman[17] and Abuaf and Staub[8] used flat copper surfaces. All these surfaces did not have the same surface finish. The transition from free convection to nucleate boiling was assumed to occur at around 6°C where the free convection curve (Eq (4)) intersects with the nucleate boiling curve (Eq (5)). This value also agrees with the transition temperature difference proposed by Dulkin et al[13]. The temperature difference at the critical heat flux limit was determined as the point of intersection of the nucleate boiling curve ($q = B(\Delta T)^{3.92}$) proposed by Stephan and Abdelsalam[16] and the critical heat flux expression derived by Zuber[9] and Kutateladze[10].

$$q_{max} = K\sqrt{\rho_g} h_{fg} (g\sigma(\rho_l - \rho_g))^{1/4} \tag{6}$$

The value of the constant K varies between 0.13 and 0.18.

The film boiling heat transfer coefficient was calculated from the minimum heat flux expression proposed by Zuber[9]:

$$q_{min} = \frac{q_{max}}{\left[\frac{\rho_l + \rho_g}{\rho_g}\right]^{1/2}} \tag{7}$$

The film boiling limit temperature difference was reported to exist between 55°C (Haley and Westwater[1]) and 72.5°C (Dulkin et al.[13]). The variation of the heat transfer coefficient in the transition region between q_{max} and q_{min} was assumed to be linear with the temperature difference. The heat transfer coefficient, as a function of temperature difference for R-113 at atmospheric pressure, is calculated using the above methodology and presented in Fig 8 as the solid thick line for $K = 0.13$ and q_{min} at 55°C.

The boiling curve heat transfer correlations presented above and compared with atmospheric pressure data in Fig 8 were used in all subsequent calculations, assuming that they properly account for the pool pressure effects.

The one-dimensional numerical results calculated with the temperature-dependent heat transfer coefficients described above are compared in Fig 9 with the fin boiling data obtained at 0.86 atm with the finned copper heater. It can be seen that the calculations underpredict the experimental results for temperature differences below 20°C and overpredict them above 20°C. The critical heat flux limits predicted vary between 60 and 90 W/cm² (depending on the value of the constant K (0.13 or 0.18) used in Eq (6) and the temperature difference at q_{min} (55 or 72.5°C)), while the measured value is 70 W/cm². The predictions will also vary with the exponent for the temperature difference used in the nucleate boiling region (Eq (5)). For the present study we limited ourselves to the 2.92 power since it appeared to predict adequately the nucleate boiling curve data reported by Abuaf and Staub[8] for plain surfaces.

In order to check any three dimensional effects that may be present in the fin performance due to the non-linearity of the heat transfer coefficients, a three-dimensional model of the quarter of the fin structure was also investigated (Fig 7(a)). The solution was obtained by using the program ADINAT, developed at MIT, by Bathe[19]. ADINAT is a commercially available finite-element program which can be used to solve conduction problems with linear and non-linear material properties and boundary conditions. Although it permits the use of

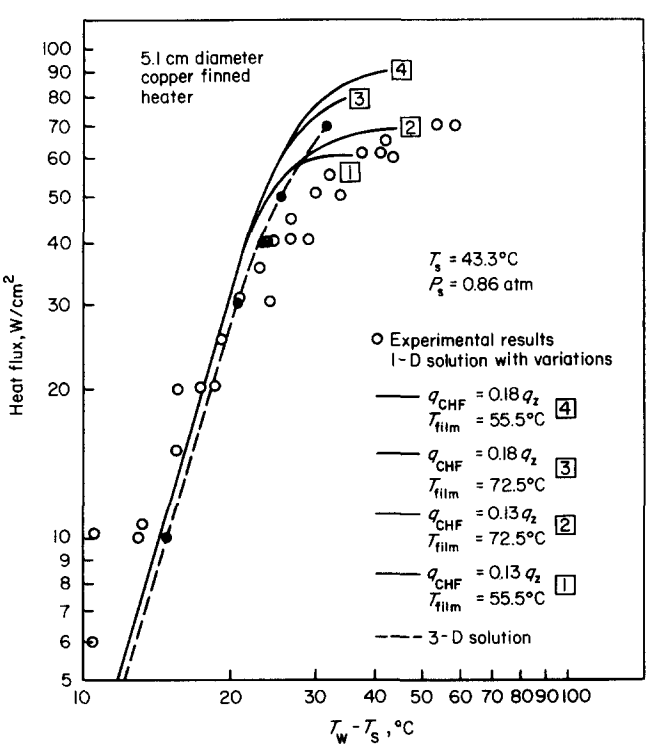

Fig 9 Comparison of results

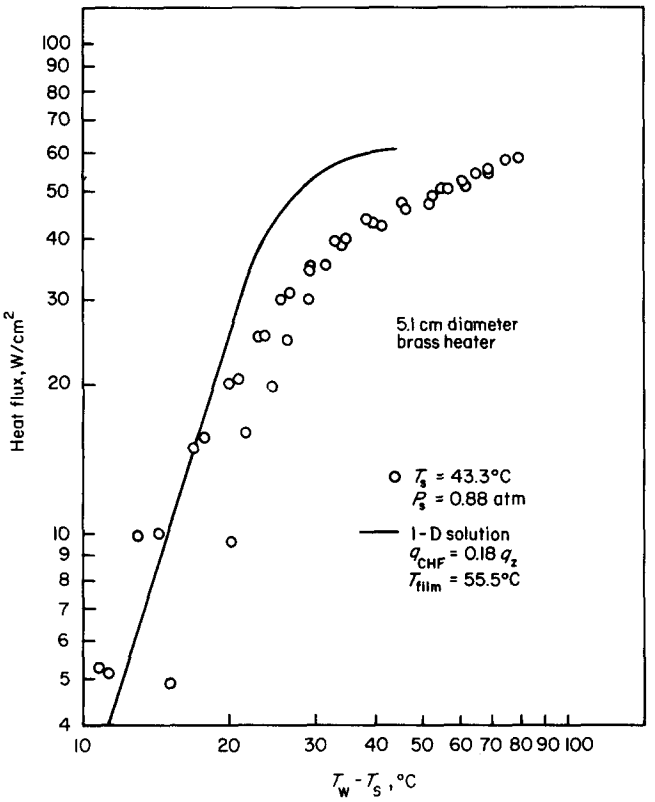

Fig 10 Results calculated for the brass heater compared with predictions

eight-noded elements, in the present calculations only four-noded elements were used. The three-dimensional calculations performed under the same conditions and presented as the dashed line in Fig 9 show that the one dimensional calculations were accurate and no significant three-dimensional effects should be expected.

In order to check the effect of the thermal conductivity of the heater material, one dimensional model results were recalculated for the brass heater (thermal conductivity equals 1.16 W/cm °C). The data are compared with the predictions ($K = 0.18$ in Eq (6) and temperature difference at film boiling 55°C) in Fig 10 for a pool saturation temperature of 43.3°C and a pressure of 0.86 atm. The boiling curve predicted shows larger temperature differences for the same heat flux than the copper finned heater. At high heat fluxes close to the critical heat flux limit the transition from nucleate boiling to CHF occurs at larger temperature differences than those obtained with the copper heater. On the other hand, the model predicts the measured critical heat flux limit of 60 W/cm^2 which is 17% lower than the one observed with the finned copper heater. The difference observed between the one-dimensional calculations and the data at temperature differences above 25°C, ie the over prediction of the heat flux for a given temperature difference, can be attributed to the temperature-dependent heat transfer coefficients used. The value of the temperature difference used at the film boiling point is 55°C which was determined from data obtained with R-113-copper rather than with R-113-brass combination. The constant B in the nucleate boiling correlation (Eq (5)) was also determined for R-113 with copper heaters and not with brass heaters. The surface finish of the brass and copper heaters is also expected to affect the nucleate boiling heat transfer coefficients.

The temperature-dependent heat transfer coefficients formulated above can not be applied to finned surfaces operating in saturated pools where the pressure is below 0.2 atm. In this region the critical heat flux limits measured with plain surfaces do not follow the hydrodynamic theories (Fig 6) and at present there is no satisfactory model to calculate them[20]. In addition the pressure dependance of the transition region, the film boiling heat flux, and the temperature difference at q_{min} for R-113 are not well documented. The one-dimensional model was used for the 0.5 atm data, since at this pressure level the critical heat flux limits of plain surfaces are still predicted by the hydrodynamic theories and the nucleate boiling curves for plain copper surfaces in R-113 reported by Abuaf and Staub[8] closely agreed with Stephan and Abdelsalam's correlation (Eq (5)). In Fig 11 the calculated results are compared with the data obtained with the 5.1 cm finned copper heater operated at 25.9°C and 0.5 atm pressure. For temperature differences below 25°C, the nucleate boiling curve predicted is much lower than the data. Above 25°C the predictions become larger than the experimental results. Although there is a considerable difference between the two boiling curves, the critical heat flux limit calculated is very close to the measured value (61 versus 60 W/cm^2). The latter agreement may well be fortuitous since Eq 6 is based on a hydrodynamic flooding criteria for plain surfaces. For the case of closely spaced

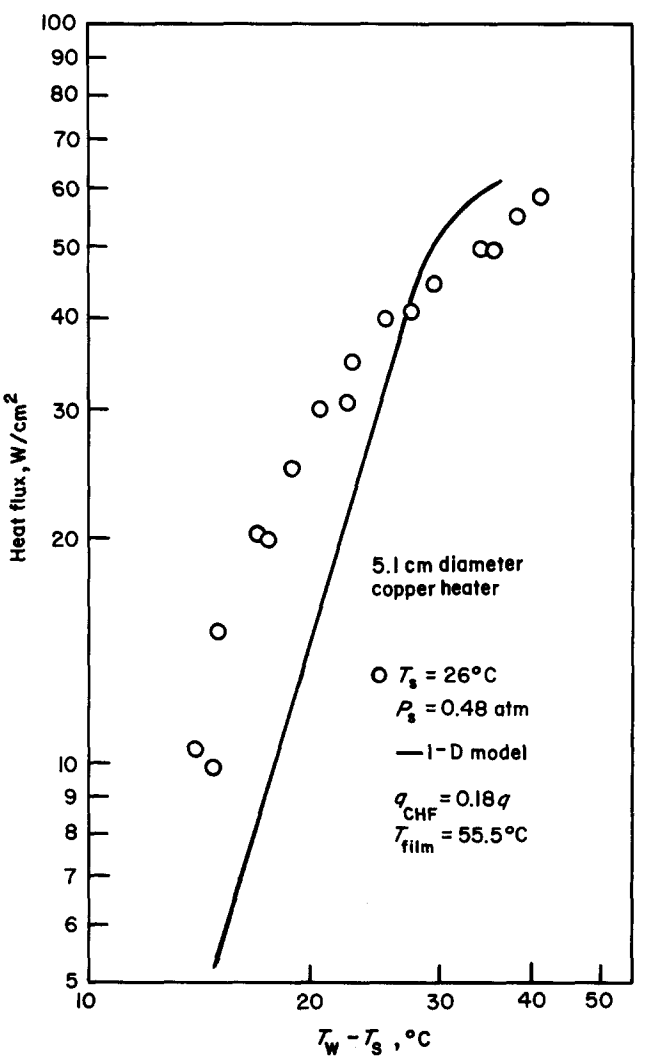

Fig 11 Calculated results compared with experimental data

fins, the hydrodynamic flooding limit may be calculated by the vapour-liquid counter flow between the fins or by the geometry of the upflowing vapour columns and downflowing liquid above the finned surface. In the latter case the fin structure could reduce the spacing between the vapour jets that would normally occur over a plain surface thus increasing the critical heat flux limit of the finned surface. In the absence of more detailed measurements of the two-phase flow patterns with closely-spaced fins, this argument for the increase in the finned critical heat flux remains a hypothesis.

Regarding the difference in the behaviour between the calculated and measured nucleate boiling curves in Fig 11 one can also hypothesize that, at low pressures, the horizontal plain surface boiling curves cannot be used for closely packed fin configurations since different boiling regimes will be expected to occur between two close vertical walls. Additional well planned experiments and modelling are necessary to clarify this question. Based on the above comparison one can conclude that although the fin calculations predict the finned surface performance close to atmospheric pressures, at present they can not be extended to subatmospheric pressures (0.5 atm). The above results show the importance of the accurate knowledge of the details of the entire boiling curve, covering all the regimes, in the application of the non-linear fin equations to boiling systems.

Conclusions

The results and conclusions derived from the present study can be summarised as:

1. Copper and brass finned structure surfaces have been investigated and boiling curves and critical heat flux limits were measured in an R-113 saturated pool in the pressure range between 1 and 0.039 atm.
2. For a given heat flux level in the nucleate boiling region, the finned surfaces have a lower temperature difference between the wall and the pool resulting in higher nucleate boiling heat transfer coefficients.
3. The critical heat flux limits for the copper finned surfaces, based on a heater projected area, are 2–2.5 times higher than those obtained with the plain copper surfaces. The critical heat flux limits measured with the brass finned surface are 15 to 20% lower than the ones obtained with the copper heater.
4. With decreasing pressure the boiling curves of finned surfaces move to higher wall-to-pool temperature differences similar to the observations reported with plain surfaces.
5. The critical heat flux limits of finned surfaces indicate a dependance on pool pressure similar to that of plain surfaces. They first decrease with pressure in the range between 0.3 and 1 atm at a similar rate as the plain surfaces. At lower pressures the dependence is less pronounced.
6. The fin equation with a non-linear heat transfer coefficient covering all the regimes in a complete boiling curve were solved to check the data. The predictions depend on the nucleate boiling heat transfer correlation, the critical heat flux limit, the transition boiling correlation, the film boiling heat flux limit as well as the temperature levels where the transitions are occuring. Thus a sound knowledge of the entire boiling curve for a given liquid-heater material combination is essential before undertaking similar predictions.
7. The calculated nucleate boiling curves for finned surfaces agree with the data for pressure levels close to atmospheric, but show important differences at subatmospheric pressures.
8. The difference between the calculations and the data at subatmospheric pressures raises the question of whether the augmentation in the nucleate boiling heat transfer coefficients and critical heat flux limits observed with finned surfaces are mainly due to conduction effects and thus can be predicted by solving the fin equation with the appropriate heat transfer coefficients for all the regimes in a typical boiling curve. The question to be answered is whether there exist additional phenomena, and effects such as a reduction of the Taylor wavelength or bubble departure diameters by the fin spacing and geometrical effects such as boiling between two closely spaced vertical walls, which affect the boiling curve correlation (the constant and the power in Eq (5)). These points were not considered in the solution of the fin equation which used the critical heat flux limit and the boiling heat transfer coefficients of a horizontal plain surface. Additional experiments and modelling are necessary in order to clarify these points if such extended surfaces are going to be used in practical applications.

References

1. **Haley K. W. and Westwater J. W.** *3rd Int. Heat Tr. Conf., vol III Chicago, 1966*
2. **Bergles A. E.** *Progress in heat and mass transfer, Vol. 1, eds. A. Grigull and E. Hahne, Pergamon Press, 1969*
3. **Bergles A. E., Junkhan G. H. and Webb R. L.** *HTL-30, ISU-ERI-Ames 83158, Iowa State Univ., 1982*
4. **Webb R L.** *Heat Transfer Engineering*, **2**, *pp 46–69, 1981*
5. **Beurtheret C.** *Revue Technique, Compagnie Francaise Thomson-Houston, No. 24, pp 56–83, 1956*
6. **Bondurant D. L. and Westwater J. W.** *Chem. Engng Progress Symp. Series, 113, pp 30–37, 1971*
7. **Westwater J. W.** *AIChE Symp. Ser., 69, 131, pp 1–9, 1973*
8. **Abuaf N. and Staub F. W.** *Heat Transfer Seattle, AICHE Symp. Series, 225, vol. 79, 35–40, 1983*
9. **Zuber N.** *Trans. ASME*, **80**, *pp 711–720, 1958*
10. **Kutateladze S. S.** *Heat Transfer Theory Fundamentals, Nauka, 1970*
11. **Rohsenow W. M.** *Developments in Heat Transfer, Ed. W. M. Rohsenow, MIT Press, Cambridge, Mass. 1964*
12. **Lai F. S. and Hsu Y. Y.** *AIChE J.*, **13**, *pp 817–821, 1967*
13. **Dulkin I. N., Rakushina N. I., Roizen L. I. and Fastovskii V. G,** *Article translated from Inzhener. Zhurnal*, **19**, *pp 637–645, 1970*
14. **Collier J. G.** *Convective boiling and condensation, McGraw Hill, 1972*
15. **Lippert T. E. and Dougall R. S.** *J. of Heat Transfer*, **90**, *pp 347–352, 1968*
16. **Stephan K. and Abdelsalam M.** *Int. J. Heat Mass Transfer*, **23**, *pp 73–87, 1980*
17. **Chapman R. H.** *ORNL-4987, Oak Ridge National Laboratory, 1974*
18. **Marto P. J. and Lepere V. J.** Pool boiling heat transfer from enhanced surfaces to dielectric fluids, *J. Heat Transfer, Trans. ASME*, **104**, *pp 292–299, 1982*
19. **Bathe J. H.** ADINAT, *Rep. No. 82448-5, MIT, 1978*
20. **Bergles A. E.** *Nuclear Safety*, **16**, *pp 29–42, 1975*